EXPERIMENTAL AND THEORETICAL INVESTIGATION OF DIFFERENCES BETWEEN A MANUFACTURED AND THE CORRESPONDING DESIGN AIRFOIL SECTION

by

Dan M. Somers

NASA Langley Research Center

Hampton, Virginia 23665, U.S.A.

SUMMARY

Templates have been taken from a fiberglass sailplane wing and a two-dimensional wind-tunnel model constructed to the coordinates of those templates. An investigation was then conducted in the Langley low-turbulence pressure tunnel, the results being compared with data taken at the University of Stuttgart for the design section, the FX 66-17AII-182. The comparison indicated that the manufactured section had slightly higher drag and slightly lower maximum lift than the design section. An interactive graphics computer program was employed to modify the manufactured section. The modified section was theoretically superior to the manufactured one although still inferior to the design.

INTRODUCTION

Research on advanced technology airfoils has received considerable attention over the past several years at the Langley Research Center. The particular airfoil tested was selected because of the availability of data from another low-turbulence wind tunnel and because it is representative of state-of-the-art, single-element, laminar airfoils of fixed geometry (i.e., no flap). A further objective was to determine the effects of practical, fiberglass construction techniques on the aerodynamic characteristics of the airfoil. Accordingly, the wind-tunnel model was built to coordinates measured from templates of a fiberglass sailplane wing. The airfoil corresponds to the FX 66-17AII-182 designed by Professor F.X. Wortmann of the University

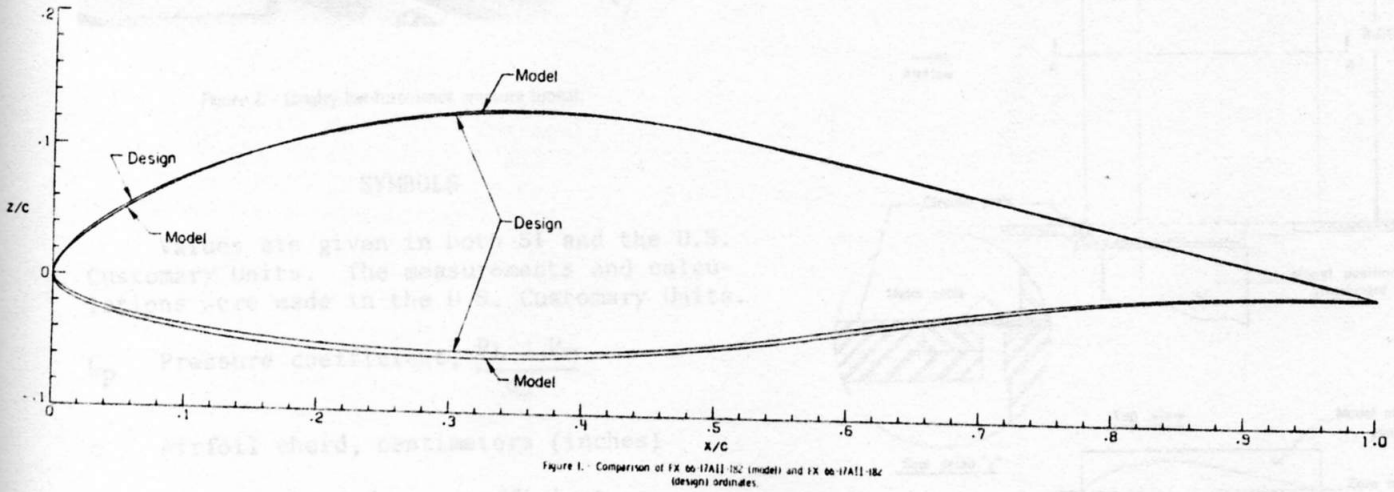

Figure 1.- Comparison of FX 66-17AII-182 (model) and FX 66-17AII-182 (design) ordinates.

of Stuttgart, West Germany. The experimental section characteristics of the FX 66-17AII-182 are reported in Reference 1.

The investigation was performed in the Langley low-turbulence pressure tunnel (LTPT) to obtain the basic low-speed, two-dimensional aerodynamic characteristics of the airfoil. The results have been compared with theoretical data generated by a viscous, subsonic airfoil computer program and with data from Reference 1. During the test, the Reynolds number, based on airfoil chord, varied from approximately 1.0×10^6 to 3.0×10^6, with geometric angle of attack ranging from -10^o to 15^o.

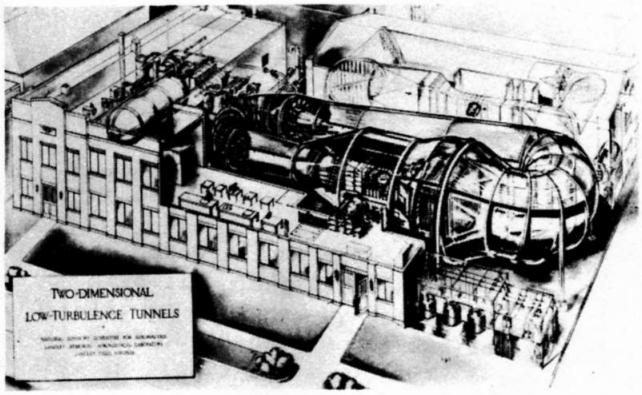

Figure 2.- Langley low-turbulence pressure tunnel.

SYMBOLS

Values are given in both SI and the U.S. Customary Units. The measurements and calculations were made in the U.S. Customary Units.

C_p Pressure coefficient, $\frac{p_L - p_\infty}{q_\infty}$

c Airfoil chord, centimeters (inches)

c_c Section chord-force coefficient, $\oint C_p \, d\left(\frac{z}{c}\right)$

c_d Section profile-drag coefficient, $\int_{wake} c'_d \, d\left(\frac{h}{c}\right)$

c'_d Point drag coefficient (Ref. 3)

c_l Section lift coefficient, $c_n \cos \alpha - c_c \sin \alpha$

c_m Section pitching-moment coefficient about quarter-chord point, $-\oint C_p \left(\frac{x}{c} - 0.25\right) d\left(\frac{x}{c}\right) + \oint C_p \left(\frac{z}{c}\right) d\left(\frac{z}{c}\right)$

c_n Section normal-force coefficient, $-\oint C_p \, d\left(\frac{x}{c}\right)$

h Vertical distance in wake profile, centimeters (inches)

M Free-stream Mach number

p Static pressure, N/m^2 (lb/ft^2)

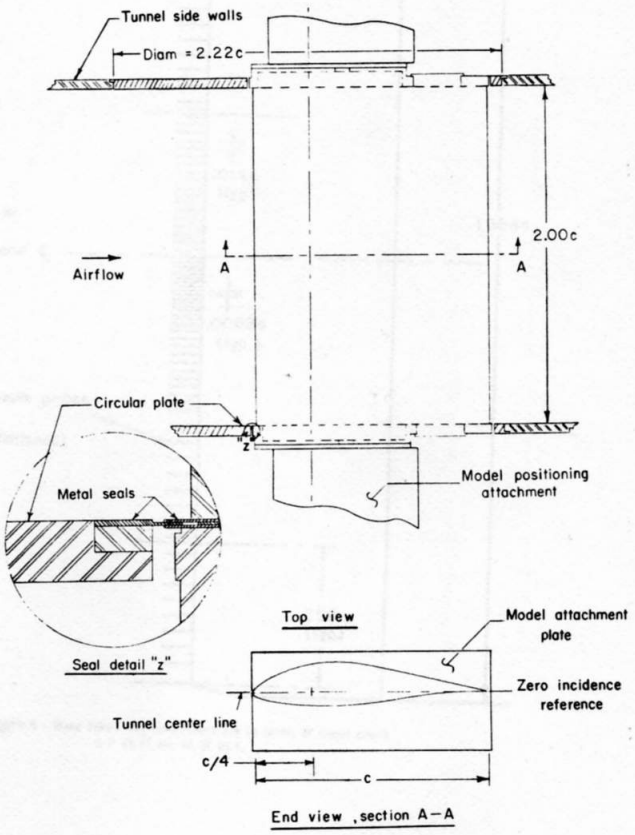

Figure 3.- Airfoil model mounted in wind tunnel. All dimensions are in terms of model chord, c = 45.77 cm (18.02 in.).

q Dynamic pressure, N/m^2 (lb/ft^2)

R Reynolds number based on free-stream conditions and airfoil chord

x Airfoil abscissa, centimeters (inches)

z Airfoil ordinate, centimeters (inches)

α Angle of attack, degrees

Subscripts:

L Local point on airfoil

max Maximum

min Minimum

T Transition

∞ Free-stream conditions

Abbreviations:

L.S. Lower surface

U.S. Upper surface

MODEL, APPARATUS, AND PROCEDURE MODEL

The coordinates of the model are listed in Table I (on page 11) along with those for the FX 66-17AII-182 as designed by Wortmann. The two airfoil section shapes, model and design, are compared in Figure 1.

The model consisted of a metal spar surrounded by plastic filler with fiberglass forming the aerodynamic surface. The model had a chord of 45.77 cm (18.02 in) and a span of 91.44 cm (36.00 in). Upper and lower surface orifices were located 2.54 cm (1.00 in) to one side of midspan at the chord stations indicated in Table II. Spanwise orifices were located in the upper surface only to monitor the two-dimensionality of the flow at high angles of attack. The model surface was sanded in the chordwise direction with number 600 dry silicon carbide paper to insure an aerodynamically smooth finish.

WIND TUNNEL

The Langley low-turbulence pressure tunnel (Ref. 2) is a closed-throat, single-return tunnel (Fig. 2) which can be operated at stagnation pressures from 10.13 to 1013 kN/m^2 (0.1 to 10 atm) with tunnel-empty, test section Mach numbers up to 0.46 and 0.23, respectively. The minimum unit Reynolds number is approximately 0.66×10^6 per meter (0.20×10^6 per ft) at a Mach number of about 0.10. The maximum unit Reynolds number is approximately 49×10^6 per meter (15×10^6 per ft) at a Mach number of 0.23. The test section is 91.44 cm (3.000 ft) wide by 228.6 cm (7.500 ft) high.

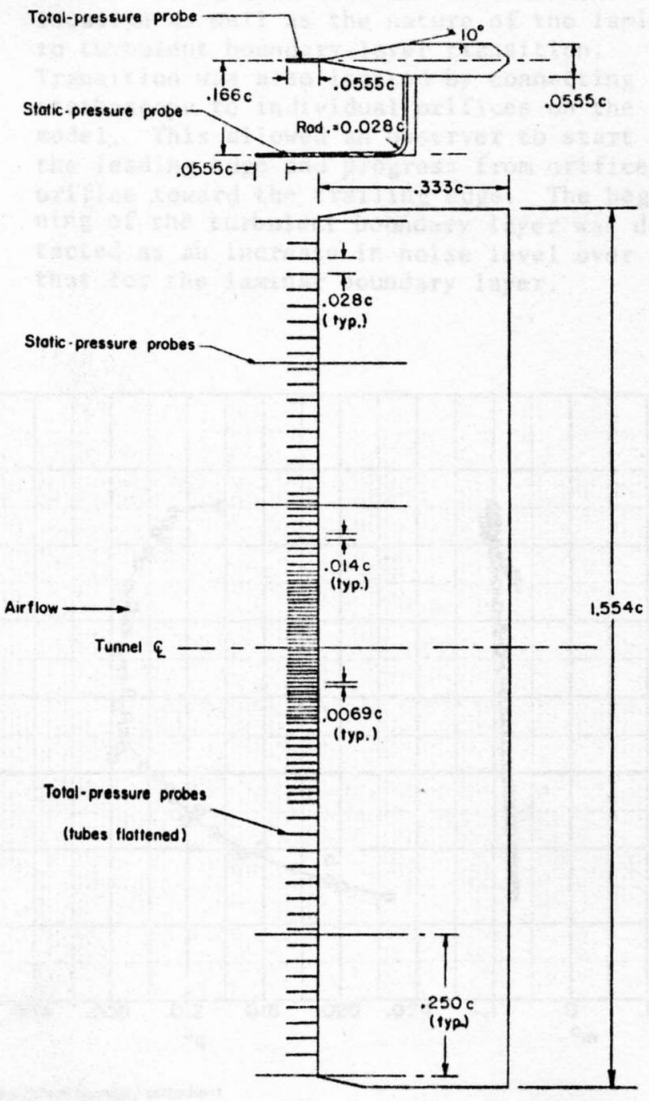

Figure 4. - Wake rake. All dimensions are in terms of model chord, c = 45.77 cm (18.02 in.).

Hydraulically actuated, circular plates provide positioning and attachment for the two-dimensional model. The plates are flush with the tunnel sidewalls, 101.6 cm (40.00 in) in diameter, and rotate with the model. The model ends were mounted to rectangular, model attachment plates (Fig. 3) such that the center of rotation of the circular plates coincided with 0.25c on the model chord line. The gaps between the rectangular plates and the circular plates were closed with flexible, sliding metal seals, as shown in Fig. 3.

WAKE SURVEY RAKE

A fixed, wake survey rake (Fig. 4) was cantilever mounted from the tunnel sidewall at the model midspan and approximately 1.6 chord lengths downstream from the trailing edge of the model. The wake rake employed 91 total-pressure tubes, 0.152 cm (0.060 in) in diameter, and five static-pressure tubes, 0.318 cm (0.125 in) in diameter. The total-pressure tubes were flattened to 0.102 cm (0.040 in) for 0.61 cm (0.24 in) from the tip of the tube. Each static-pressure tube had four flush orifices located 90° apart, eight tube diameters from the tip of the tube in the measurement plane of the total-pressure tubes.

INSTRUMENTATION

Measurements of the static pressures on the model surfaces and the wake rake pressures were made by an automatic, pressure-scanning system utilizing variable-capacitance-type, precision transducers. Basic tunnel pressures were measured with precision quartz manometers. Angle of attack was measured by a calibrated, digital shaft encoder driven by a pinion gear and rack attached to the circular plates. Data were obtained by a high-speed, data-acquisition system and recorded on magnetic tape.

TESTS AND METHODS

For several test runs, the model upper surface was coated with oil to determine the location as well as the nature of the laminar to turbulent boundary-layer transition. Transition was also located by connecting a stethoscope to individual orifices on the model. This allowed an observer to start at the leading edge and progress from orifice to orifice toward the trailing edge. The beginning of the turbulent boundary layer was detected as an increase in noise level over that for the laminar boundary layer.

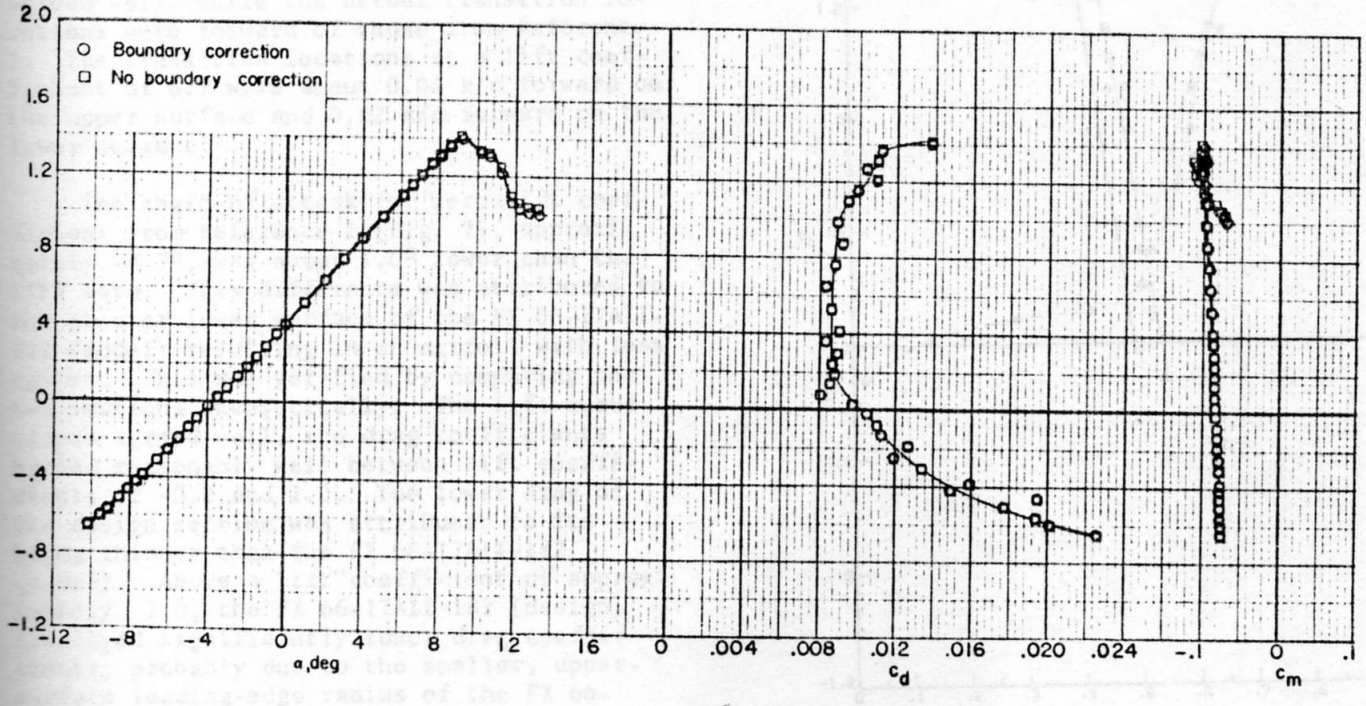

Figure 5. - Effect of standard low-speed wind tunnel boundary corrections on section data. $R \approx 1.5 \times 10^6$, $M = 0.10$.

The static-pressure measurements at the airfoil surface were reduced to standard pressure coefficients and machine integrated to obtain section normal-force and chord-force coefficients and section pitching-moment coefficients about the quarter chord. Section profile-drag coefficients were computed from the wake-rake total and the tunnel sidewall static pressures by the method of Reference 3. The tunnel sidewall static pressures were used instead of the wake-rake static pressures because the rake cannot be alined with the flow in the wake.

An estimate of the standard low-speed, wind-tunnel boundary corrections (Ref. 4) is shown in Figure 5. The corrections, approximately 1 percent of the measured coefficients, have been applied to the data.

DISCUSSION

Experimental Results

Comparison With Other Data. The variation of lift coefficient with transition location at a Reynolds number of approximately 1.5×10^6 compared favorably with the data for the FX 66-17AII-182 (design) (Fig. 6) from Reference 1. The rates of variation agreed well, while the actual transition locations were forward of those from Reference 1. The transition locations at a lift coefficient of 0.7 were about 0.04 x/c forward on the upper surface and 0.02 x/c forward on the lower surface.

The angle of attack for zero lift coefficient from Reference 1 (Fig. 7), approximately -4.7°, was about 1.0° lower than the LTPT data. This difference was attributed to the thicker lower surface of the FX 66-17AII-182 (model) resulting in an airfoil with less camber. This was verified by comparing the two sections theoretically. The lift-curve slopes agreed well. The drag coefficients agreed reasonably well between lift coefficients of -0.2 and 1.0. The lower drag of the design section was attributed to its being thinner than the FX 66-17AII-182 (model). Above a lift coefficient of approximately 1.0, the FX 66-17AII-182 (design) displayed significantly lower drag coefficients, probably due to the smaller, upper-surface leading-edge radius of the FX 66-17AII-182 (model). (See Fig. 1.) The smaller radius developed a leading-edge pressure peak earlier, resulting in forward movement of the transition location at a lower lift coefficient. This also accounts for the lower maximum lift coefficient. The pitching-moment coefficients agreed well for the two sections.

COMPARISON OF EXPERIMENTAL AND THEORETICAL DATA

A viscous-flow airfoil method (Reference 5) was used to calculate two chord-wise pressure distributions corresponding to data taken in the current wind-tunnel investigation. The theory agreed quite well with experiment over the entire chord (Fig. 8) with the major discrepancies occurring at locations corresponding to laminar separation bubbles.

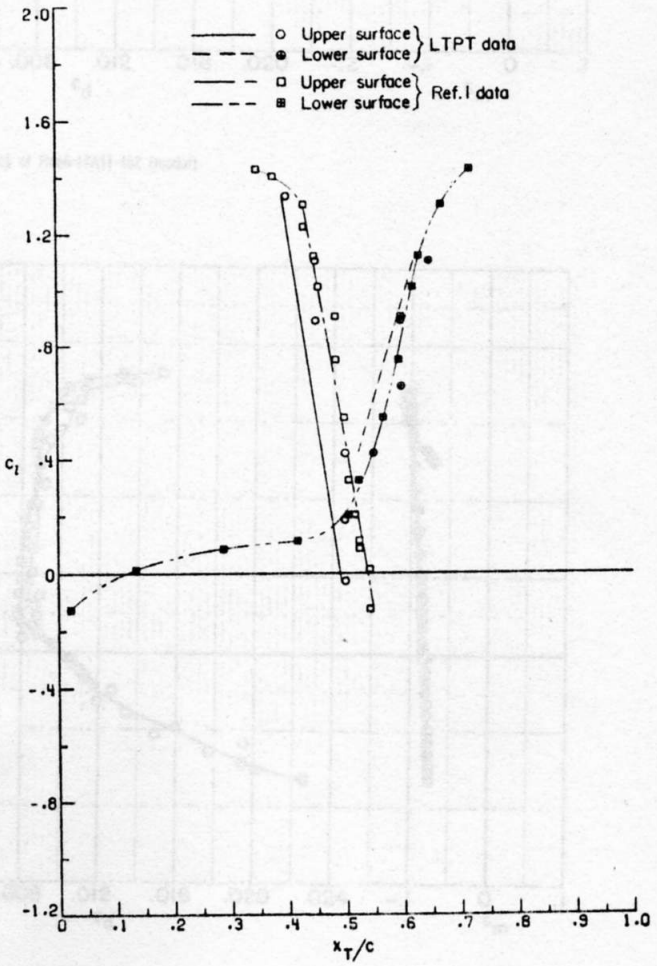

Figure 6.- Comparison of transition location on FX 66-17AII-182 (model) and FX 66-17AII-182 (design). $R = 1.5 \times 10^6$.

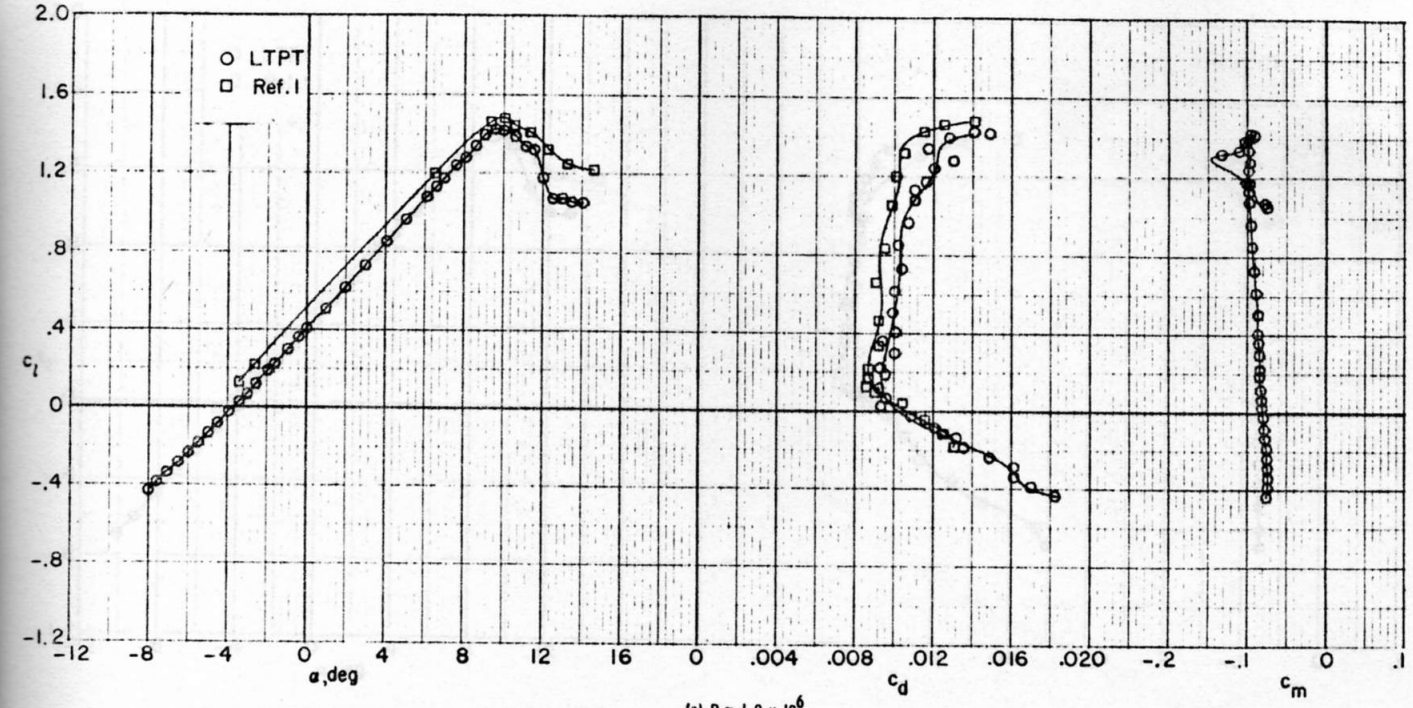

(a) $R \approx 1.0 \times 10^6$.

Figure 7. - Comparison of section characteristics of FX66-17AII-182 (model) and FX66-17AII-182 (design).

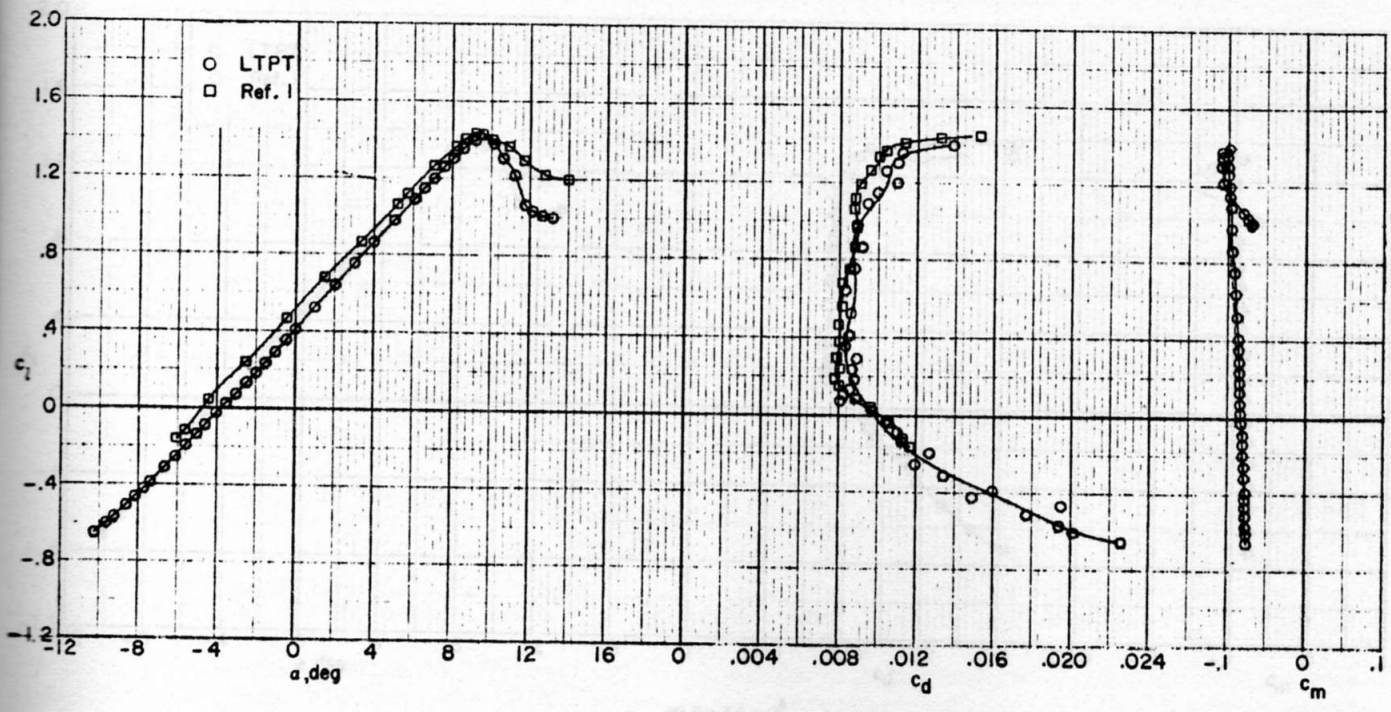

(b) $R \approx 1.5 \times 10^6$.

Figure 7. - Continued.

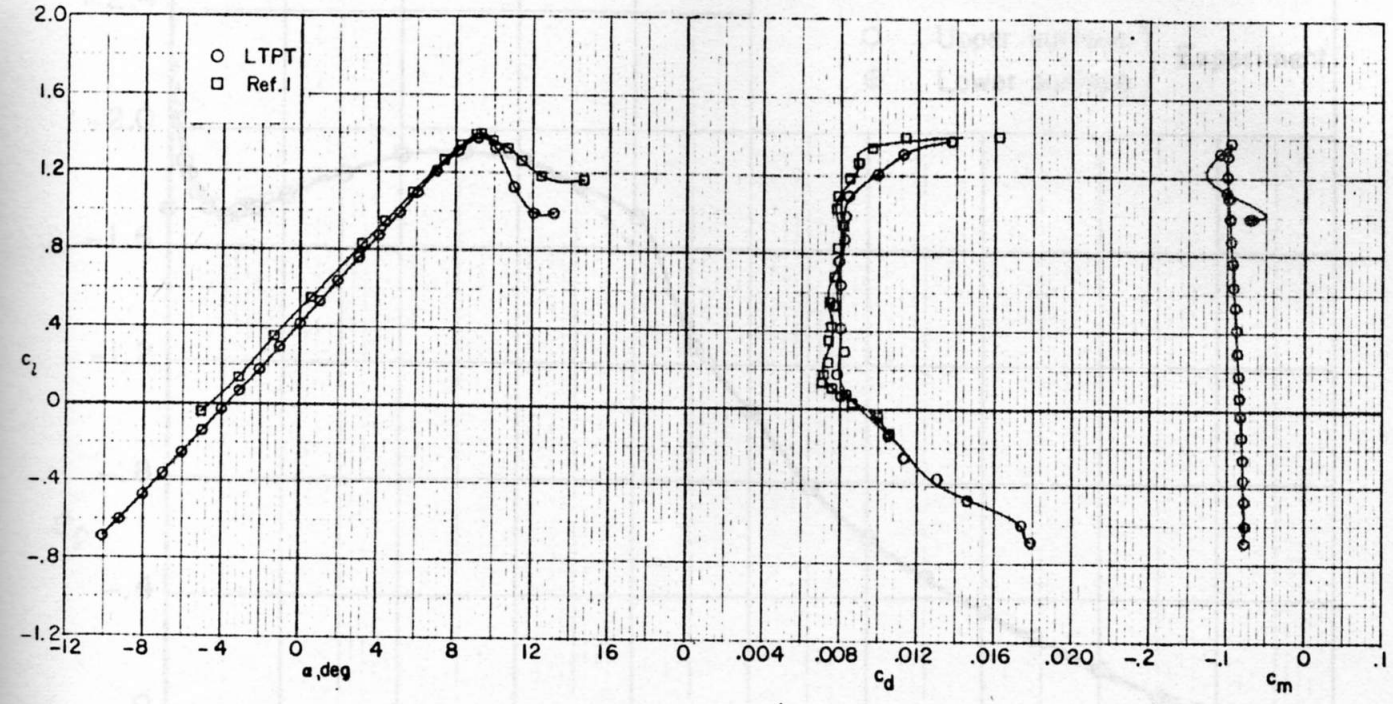

(c) $R \approx 2.0 \times 10^6$.

Figure 7. - Continued.

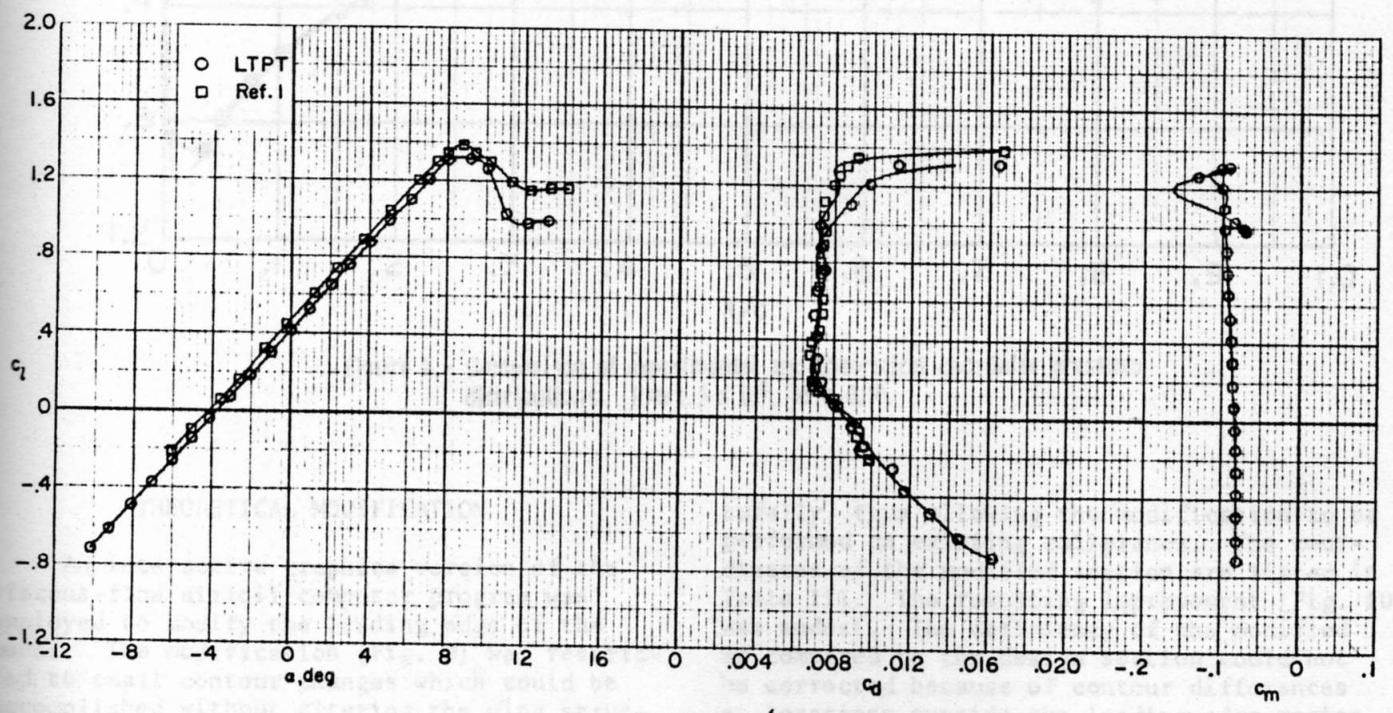

(d) $R \approx 3.0 \times 10^6$.

Figure 7. - Concluded.

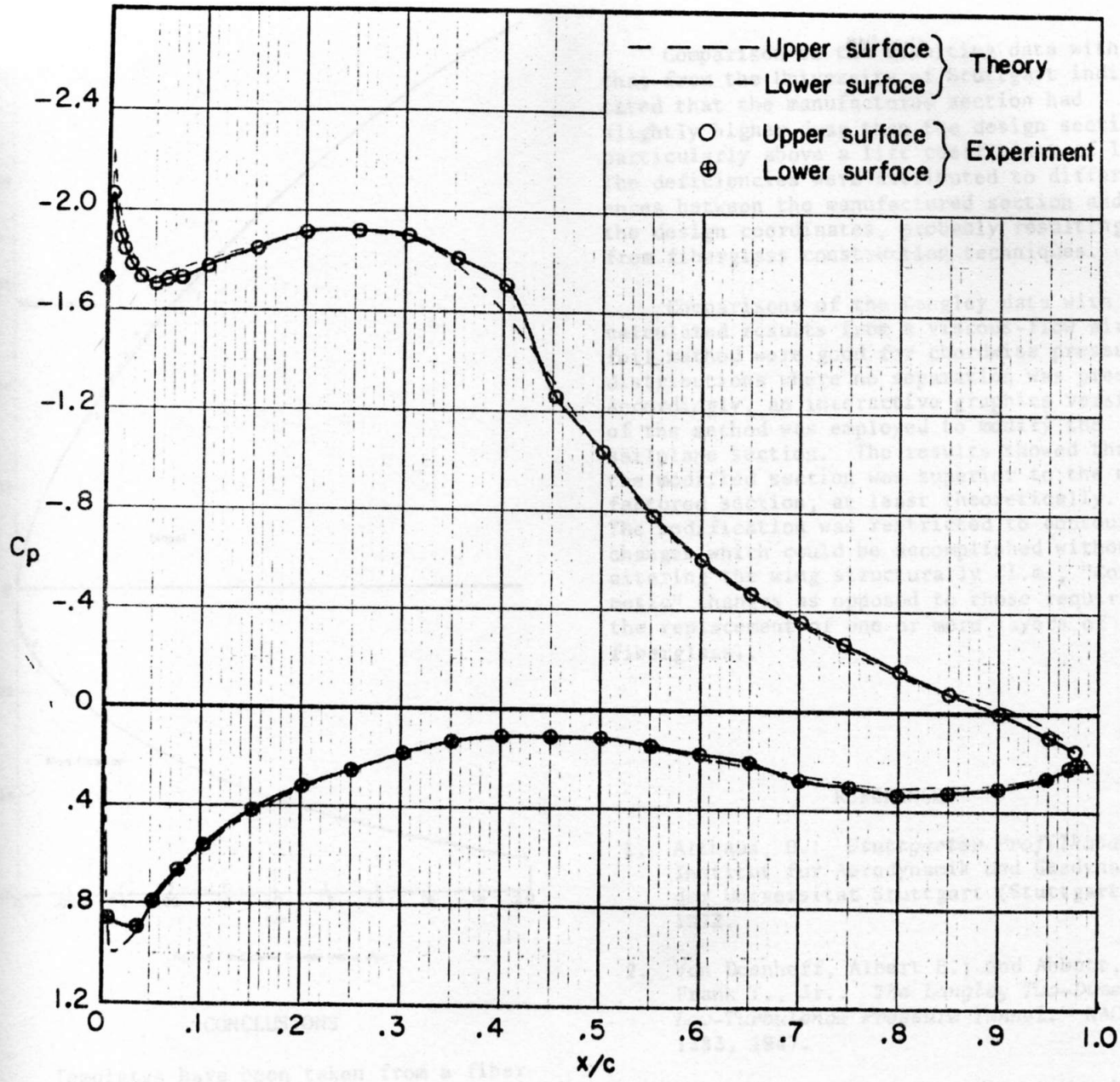

Figure 8.- Comparison of experimental and theoretical chordwise pressure distributions. $R \approx 1.5 \times 10^6$, $M = 0.10$.

THEORETICAL MODIFICATION

An interactive graphics version of the viscous-flow airfoil computer program was employed to modify the leading edge of the model. The modification (Fig. 9) was restricted to small contour changes which could be accomplished without altering the wing structurally, thus allowing the modification to be performed on existing sailplanes. The coordinates of the modified section are listed in Table III. The resulting improvement (Fig. 10) was modest. The deficiency of the modified as compared to the design section could not be corrected because of contour differences at locations outside the leading-edge region

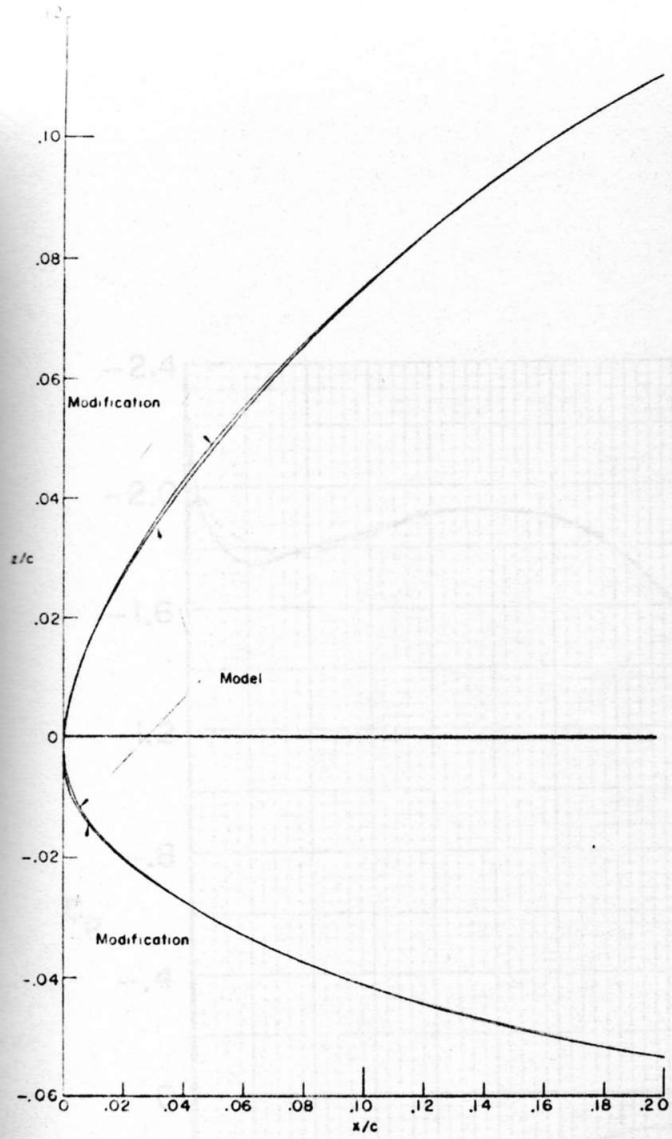

Figure 9. - Modification to model leading edge.

CONCLUSIONS

Templates have been taken from a fiberglass sailplane wing and a wind-tunnel model constructed to the coordinates of those templates. An investigation was then conducted in the Langley low-turbulence pressure tunnel to determine the basic low-speed, two-dimensional aerodynamic characteristics of the airfoil, which corresponds to the FX 66-17AII-182 designed by Professor F.X. Wortmann. The results were compared with data taken at the University of Stuttgart for the design coordinates and with theoretical calculations using a viscous-flow airfoil method. The tests were performed at Reynolds numbers, based on airfoil chord, from approximately 1.0×10^6 to 3.0×10^6.

Comparison of the resulting data with that from the University of Stuttgart indicated that the manufactured section had slightly higher drag than the design section, particularly above a lift coefficient of 1.0. The deficiencies were attributed to differences between the manufactured section and the design coordinates, probably resulting from fiberglass construction techniques.

Comparisons of the Langley data with calculated results from a viscous-flow airfoil method were good for chordwise pressure distributions where no separation was present. Accordingly, an interactive graphics version of the method was employed to modify the sailplane section. The results showed that the modified section was superior to the manufactured section, at least theoretically. The modification was restricted to contour changes which could be accomplished without altering the wing structurally (i.e., "Cosmetic" changes as opposed to those requiring the replacement of one or more layers of fiberglass).

REFERENCES

1. Althaus, D.: *Stuttgarter Profilkatalog I.* Institut fur Aerodynamik und Gasdynamik der Universitat Stuttgart (Stuttgart), 1972.

2. Von Doenhoff, Albert E.; and Abbott, Frank T., Jr.: *The Langley Two-Dimensional Low-Turbulence Pressure Tunnel.* NACA TN 1283, 1947.

3. Pankhurst, R.C.; and Holder, D.W.: *Wind-Tunnel Technique.* Sir Isaac Pitman & Sons, Ltd. (London), 1952.

4. Allen, H. Julian; and Vincenti, Walter G.: *Wall Interference in a Two-Dimensional-Flow Wind Tunnel, With Consideration of the Effect of Compressibility.* NACA Rep. 782, 1944.

5. Smetana, Frederick O.; Summey, Delbert C.: Smith, Neill S.; and Carden, Ronald K.: *Light Aircraft Lift, Drag, and Moment Prediction — A Review and Analysis.* NASA CR-2523, 1975.

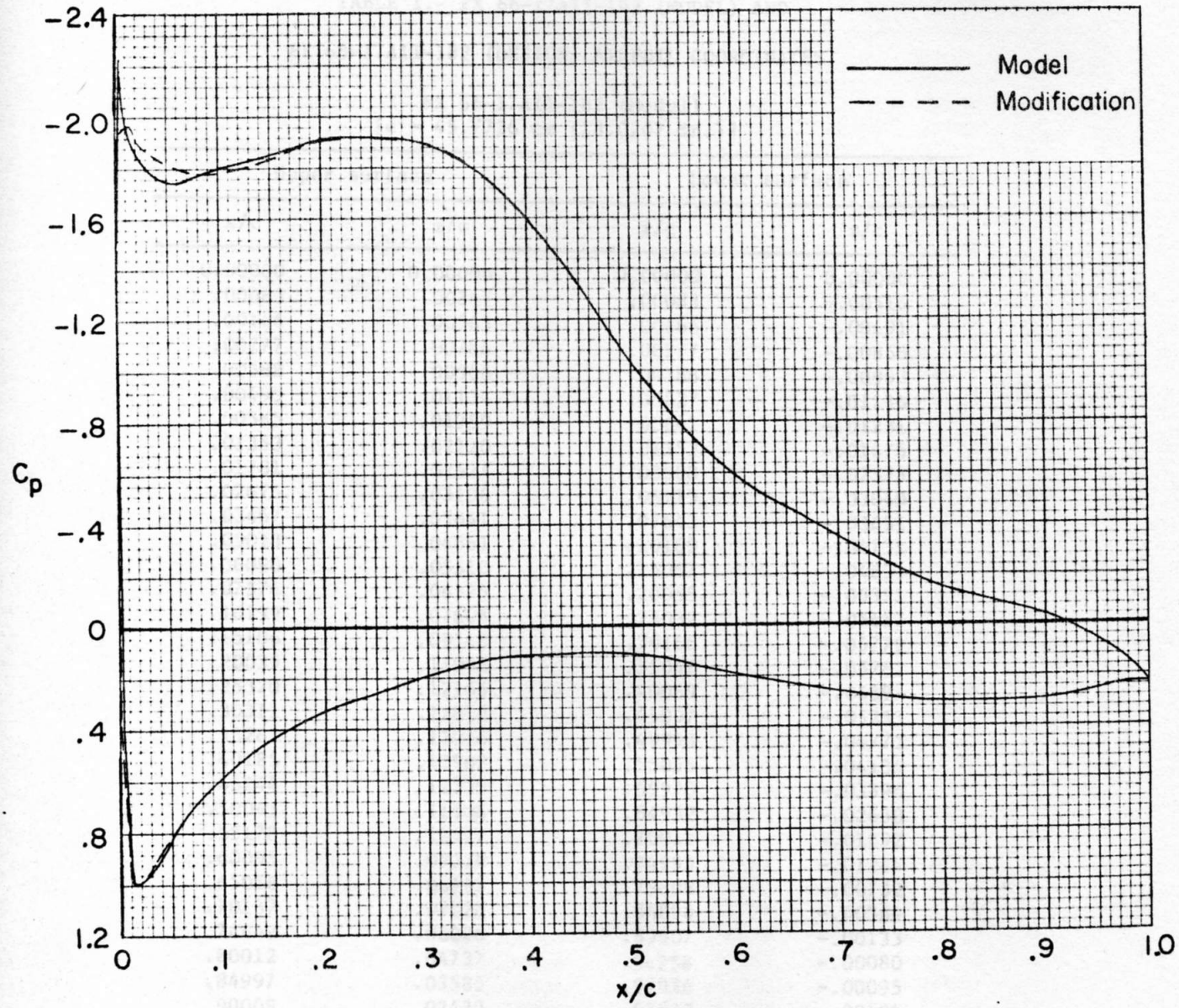

Figure 10. - Comparison of model and modification theoretical chordwise pressure distributions. $R \approx 1.5 \times 10^6$, $M = 0.10$, $c_l = 1.293$.

TABLE I.- FX 66-17AII-182 (MODEL) AND

FX 66-17AII-182 (DESIGN) AIRFOIL COORDINATES

FX 66-17AII-182 (Model)
[c = 45.7726 cm (18.0207 in.)]

Upper surface		Lower surface	
x/c	z/c	x/c	z/c
0.00000	0.00000	0.00000	0.00000
.00083	.00347	.00083	-.00516
.00166	.00563	.00166	-.00691
.00277	.00786	.00277	-.00856
.00388	.00966	.00388	-.00992
.00499	.01134	.00527	-.01136
.00585	.01259	.00641	-.01231
.01353	.02120	.01352	-.01676
.01781	.02521	.03588	-.02573
.02475	.03106	.05113	-.03040
.03467	.03841	.07643	-.03651
.05013	.04861	.10169	-.04131
.06090	.05510	.15067	-.04833
.07574	.06328	.20055	-.05321
.10199	.07608	.25032	-.05617
.15106	.09548	.30166	-.05779
.20035	.11042	.35047	-.05782
.25320	.12165	.40069	-.05597
.30311	.12819	.45007	-.05253
.35283	.13066	.49998	-.04772
.40185	.12902	.55056	-.04134
.45244	.12335	.59970	-.03396
.50043	.11506	.64952	-.02630
.55178	.10427	.70012	-.01892
.60095	.09328	.74995	-.01234
.65056	.08197	.79808	-.00732
.70137	.07028	.84898	-.00364
.74442	.06026	.89907	-.00133
.80012	.04737	.94758	-.00080
.84997	.03585	.97026	-.00095
.90009	.02433	.97832	-.00104
.94994	.01257	1.00000	-.00059
.97613	.00629		
.99033	.00285		
.99964	.00021		

TABLE I.- FX 66-17AII-182 (MODEL) AND

FX 66-17AII-182 (DESIGN) AIRFOIL COORDINATES - Concluded

FX 66-17AII-182 (Design)

Upper surface		Lower surface	
x/c	z/c	x/c	z/c
0.00000	0.00000	0.00000	0.00000
.00107	.00616	.00107	-.00340
.00428	.01211	.00428	-.00741
.00961	.01866	.00961	-.01158
.01704	.02686	.01704	-.01514
.02653	.03492	.02653	-.01911
.03806	.04335	.03806	-.02298
.05156	.05201	.05156	-.02674
.06699	.06076	.06699	-.03035
.08427	.06949	.08427	-.03379
.10332	.07805	.10332	-.03702
.12408	.08635	.12408	-.04004
.14645	.09426	.14645	-.04280
.17033	.10169	.17033	-.04532
.19562	.10850	.19562	-.04752
.22221	.11460	.22221	-.04944
.25000	.11984	.25000	-.05098
.27866	.12409	.27866	-.05218
.30866	.12705	.30866	-.05292
.33928	.12874	.33928	-.05321
.37059	.12897	.37059	-.05288
.40245	.12774	.40245	-.05198
.43474	.12492	.43474	-.05037
.46730	.12065	.46730	-.04796
.50000	.11512	.50000	-.04464
.53270	.10873	.53270	-.04050
.56526	.10185	.56526	-.03573
.59755	.09476	.59755	-.03072
.62941	.08755	.62941	-.02575
.66072	.08032	.66072	-.02112
.69134	.07315	.69134	-.01693
.72114	.06614	.72114	-.01326
.75000	.05934	.75000	-.01010
.77779	.05282	.77779	-.00744
.80438	.04662	.80438	-.00522
.82967	.04078	.82967	-.00342
.85355	.03531	.85355	-.00201
.87592	.03026	.87592	-.00097
.91573	.02139	.91573	.00019
.94844	.01396	.94844	.00063
.97347	.00759	.97347	.00068
.99039	.00258	.99039	.00051
.99893	.00016	.99893	.00016
1.00000	.00000	1.00000	.00000

TABLE II.- MODEL ORIFICE LOCATIONS

Upper surface		Lower surface	
x/c	z/c	x/c	z/c
0.00000	0.00000	0.00000	0.00000
.00585	.01259	.00641	-.01231
.01353	.02120	.03588	-.02573
.01781	.02521	.05113	-.03040
.02475	.03106	.07643	-.03651
.03467	.03841	.10169	-.04131
.05013	.04861	.15067	-.04833
.06090	.05510	.20055	-.05321
.07574	.06328	.25032	-.05617
.10199	.07608	.30166	-.05779
.15106	.09548	.35047	-.05782
.20035	.11042	.40069	-.05597
.25320	.12165	.45007	-.05253
.30311	.12819	.49998	-.04772
.35283	.13066	.55056	-.04134
.40185	.12902	.59970	-.03396
.45244	.12335	.64952	-.02630
.50043	.11506	.70012	-.01892
.55178	.10427	.74995	-.01234
.60095	.09328	.79808	-.00732
.65056	.08197	.84898	-.00364
.70137	.07028	.89907	-.00133
.74442	.06026	.94758	-.00080
.80012	.04737	.97026	-.00095
.84997	.03585	.97832	-.00104
.90009	.02433		
.94994	.01257		
.97613	.00629		
.99033	.00285		

TABLE III.- COORDINATES OF MODIFIED FX 66-17AII-182 (MODEL)

Upper surface		Lower surface	
x/c	z/c	x/c	z/c
0.00000	-0.00400	0.00000	-0.00400
.00083	.00250	.00083	-.00700
.00166	.00480	.00166	-.00850
.00277	.00717	.00277	-.01000
.00388	.00925	.00388	-.01105
.00499	.01100	.00527	-.01222
.00585	.01225	.00641	-.01305
.01353	.02150	.01352	-.01725
.01781	.02575	.03588	-.02590
.02475	.03175	.05113	-.03040
.03467	.03940	.07643	-.03651
.05013	.04960	.10169	-.04131
.06090	.05585	.15067	-.04833
.07574	.06385	.20055	-.05321
.10199	.07630	.25032	-.05617
.15106	.09550	.30166	-.05779
.20035	.11042	.35047	-.05782
.25320	.12165	.40069	-.05597
.30311	.12819	.45007	-.05253
.35283	.13066	.49998	-.04772
.40185	.12902	.55056	-.04134
.45244	.12335	.59970	-.03396
.50043	.11506	.64952	-.02630
.55178	.10427	.70012	-.01892
.60095	.09328	.74995	-.01234
.65056	.08197	.79808	-.00732
.70137	.07028	.84898	-.00364
.74442	.06026	.89907	-.00133
.80012	.04737	.94758	-.00080
.84997	.03585	.97026	-.00095
.90009	.02433	.97832	-.00104
.94994	.01257	1.00000	-.00059
.97613	.00629		
.99033	.00285		
.99964	.00021		